Current Biology 24, 333–339, February 3, 2014 ©2014 Elsevier Ltd All rights reserved http://dx.doi.org/10.1016/j.cub.2013.12.041

Report

Entrainment of Brain Oscillations by Transcranial Alternating Current Stimulation

Randolph F. Helfrich,[1,*] Till R. Schneider,[1] Stefan Rach,[2,3] Sina A. Trautmann-Lengsfeld,[1] Andreas K. Engel,[1,4] and Christoph S. Herrmann[2,3,4]
[1]Department of Neurophysiology and Pathophysiology, University Medical Center Hamburg-Eppendorf, 20246 Hamburg, Germany
[2]Experimental Psychology Lab, Center for Excellence "Hearing4all," European Medical School, University of Oldenburg, 26111 Oldenburg, Germany
[3]Research Center Neurosensory Science, University of Oldenburg, 26111 Oldenburg, Germany

Summary

Novel methods for neuronal entrainment [1–4] provide the unique opportunity to modulate perceptually relevant brain oscillations [5, 6] in a frequency-specific manner and to study their functional impact on distinct cognitive functions. Recently, evidence has emerged that tACS (transcranial alternating current stimulation) can modulate cortical oscillations [7–9]. However, the study of electrophysiological effects has been hampered so far by the absence of concurrent electroencephalogram (EEG) recordings. Here, we applied 10 Hz tACS to the parieto-occipital cortex and utilized simultaneous EEG recordings to study neuronal entrainment during stimulation. We pioneer a novel approach for simultaneous tACS-EEG recordings and successfully separate stimulation artifacts from ongoing and event-related cortical activity. Our results reveal that 10 Hz tACS increases parieto-occipital alpha activity and synchronizes cortical oscillators with similar intrinsic frequencies to the entrainment frequency. Additionally, we demonstrate that tACS modulates target detection performance in a phase-dependent fashion highlighting the causal role of alpha oscillations for visual perception.

Results

In order to study the immediate electrophysiological effects of transcranial alternating current stimulation (tACS), we analyzed simultaneously recorded electroencephalogram (EEG) in 14 participants (Figure 1E). We employed a well-established visual oddball paradigm (Figure 1A) in order to retrieve highly predictable event-related potential (ERP) components [12]. To study phase-dependent effects, we delivered the visual stimulus relative to four different phase angles of the tACS wave (Figure 1B). A sham session always preceded the stimulation session to avoid carryover effects (Figure 1C). All participants received 1,000 μA stimulation intensity at 10 Hz for 20 min. Based on a previously published finite-element model of the current flow (Figure 1D) [11], we predicted that our tACS layout should induce the highest current densities in medial parieto-occipital cortex.

Retrieval of EEG Activity and ERP Components

We pioneered a novel approach for artifact removal (Supplemental Experimental Procedures available online) to remove the tACS artifact, which ideally would be removed by subtracting a constant sine wave fitted to the recordings. However, due to slight signal variations this approach did not yield satisfactory results. In order to account for the non-stationary characteristic of the recordings, we utilized a two-step procedure. First, an artifact template, comprising several adjacent artifact segments, was subtracted from every artifact segment (moving average approach). In a second step, remaining artifacts were captured by principal component analysis (PCA; Figure S1). In order to assess the impact of the artifact removal approach on the true EEG signals, we introduced a simulation approach (Supplemental Experimental Procedures) by adding a constant 10 Hz sine wave with similar characteristics to the sham data (Figure 2A, II). In order to quantify the impact of the artifact rejection on ongoing power, we compared the mean spectral power after fast Fourier transform (FFT) of the baseline sham condition (Figure 2A, I) to the artifact-corrected sham data for three frequency bands of interest (delta/theta: 1–6 Hz, alpha: 8–12 Hz, beta: 13–30 Hz). We found that the first correction step was insufficient to recover the original data in the alpha band because cleaned data and original data were significantly different (Figure 2A, III; $t_{13} = -8.56$, $p < 0.0005$, paired t test), but it was successful after the second step (Figure 2A, IV; $t_{13} = 0.5$, $p = 0.6$). Subsequently, we applied the same approach to the tACS-EEG data (Figure 2B, I) and obtained an artifact-cleaned recording (Figure 2B, III). The comparison to the alpha power in the baseline sham condition ($t_{13} = -3.74$, $p < 0.005$) indicated that neuronal activity was modulated in the alpha band and was not related to residual stimulation artifacts. Our results also suggest that true brain activity was recovered in the delta/theta band (cleaned sham: $t_{13} = 0.58$, $p = 0.57$; cleaned stimulation data: $t_{13} = -2.02$, $p = 0.06$) and the beta band (cleaned sham data: $t_{13} = -1.14$, $p = 0.28$, cleaned stimulation data: $t_{13} = -1.15$, $p = 0.27$). In addition, we also retrieved ERPs and their respective topographies (Figures 2C and 2D; Supplemental Experimental Procedures).

Power of Ongoing Activity Is Modulated by 10 Hz tACS

Although the power spectrum in the alpha band was broadly distributed during sham (Figure 3A), the peak (Figure 3B) and shape (Supplemental Experimental Procedures) were clearly modulated by stimulation. We analyzed the absolute power values with a three-way repeated-measures ANOVA (Greenhouse-Geisser corrected) with the factor *condition* (sham or stimulation), *frequency* (delta/theta: 1–6 Hz, alpha: 8–12 Hz, beta: 13–30 Hz), and *time* (pre, ISI [interstimulus interval] ±500 ms around T_0 [Figure 1B], post). We found a significant influence of the factor *frequency* ($F_{1.3,16.2} = 68.03$, $p < 0.0005$), along with a significant effect of the factor *time* ($F_{1.2,16} = 5.06$, $p < 0.05$). The factor *condition* was not significant ($F_{1,13} = 0.06$, $p = 0.8$). However, the crucial interactions of *condition* × *frequency* ($F_{1.5,19.7} = 33.54$, $p < 0.0005$), *time* × *frequency* ($F_{2,26.5} = 5.3$, $p < 0.05$), and

[4]These authors contributed equally to this work
*Correspondence: r.helfrich@uke.de

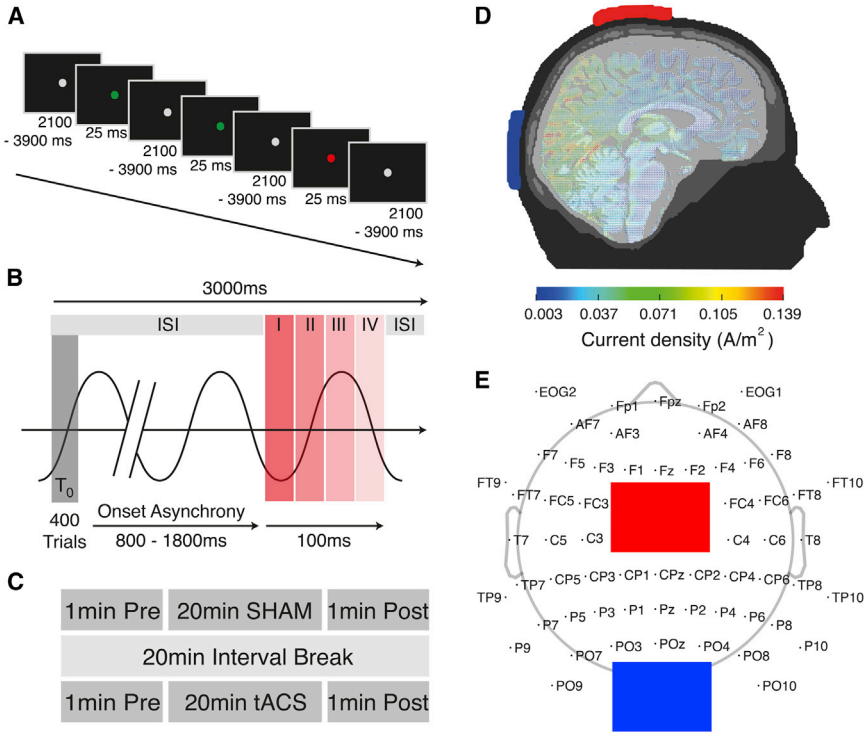

Figure 1. Experimental Setup and Procedure

(A) Oddball stimulus. Subjects were asked to fixate an LED that displayed the target color (red or green, counterbalanced across subjects) in 20% of all trials and the standard color in the remaining 80%. Subjects indicated the appearance of targets and standards by pressing different buttons.

(B) Every visual stimulus was presented for 25 ms at different phase angles of the 10 Hz tACS wave to cover the maximum, the minimum and both zero crossings followed by a variable interstimulus interval (~2,100 to ~3,900 ms). All trials were pseudorandomized, resulting in 100 trials per phase angle. A tACS trigger at T_0 was recorded every 30 cycles (=3,000 ms; during sham a faked trigger was inserted to mimic the time course of the experiment). The visual stimulus was presented following a variable onset asynchrony (800–800 ms) after T_0.

(C) Experimental procedure. The sham block always preceded the simulation block to avoid carryover effects of the tACS, which can outlast stimulation offset by over 30 min [10]. Each session was initiated and closed with 1 min of resting-state EEG during fixation of the disabled LED.

(D) The result of a finite-element model simulation of current flow from a recent publication [11], revealing the highest current flow in parieto-occipital cortex. Stimulation electrodes were positioned over Cz and Oz (international 10/20 system). Reprinted with permission of the authors.

(E) EEG and tACS electrode placement on the scalp.

condition × *frequency* × *time* ($F_{2.6,33.5} = 35.3$, $p < 0.0005$) were significant, but not *condition* × *time* ($F_{1.2,14.9} = 2.7$, $p = 0.12$). During stimulation as compared to prestimulation, we found increased alpha power compared to theta- ($F_{1,13} = 76.1$, $p < 0.0005$, planned contrast) as well as compared to beta-band power ($F_{1,13} = 68.2$, $p < 0.0005$; Table S1).

Outlasting effects of the stimulation on the alpha band (Figures 3C and 3D) were assessed with a two-way repeated-measures ANOVA with the factors *condition* (sham and stimulation) and *time* (pre and post). We found a highly significant influence of the factors *condition* ($F_{1,13} = 19.08$, $p < 0.005$) and *time* ($F_{1,13} = 20.24$, $p < 0.005$). Importantly, their *interaction* was also significant ($F_{1,13} = 8.5$, $p < 0.05$; Figures 3C and 3D), indicating that the alpha power increase was amplified during stimulation. We did not find any outlasting effects in adjacent frequency bands (all $p > 0.05$; Supplemental Experimental Procedures).

Figure 3E indicates that the peak of the alpha band is shifted during stimulation toward the stimulation frequency of 10 Hz (Levene's test for equality of variances between the sham and stimulation: $F_{1,26} = 29.6$, $p < 0.0005$).

In addition, we found a significant correlation between the alpha power during stimulation and the relative increase in alpha power after stimulation ($r = 0.58$, $p < 0.05$), but not with power before sham ($r = 0.07$, $p = 0.8$, Figure 3F) or before stimulation ($r = 0.38$, $p = 0.17$), indicating that the tACS-induced power enhancement did outlast stimulation offset (Figure 3G). Furthermore, we evaluated whether participants with a presham individual alpha frequency (IAF) of 10 Hz exhibited the strongest poststimulation power increase but did not find any evidence for this consideration (Figures 3H and S2).

tACS Effects on the Phase of Ongoing Activity

Neuronal entrainment as the basis for the increase in parieto-occipital alpha power (Figures 3A and 3B) would require the direct interaction between the external oscillatory source and an internal oscillator through synchronization [2]. Therefore, we analyzed phase-locking values (PLVs; Supplemental Experimental Procedures) between the tACS signal and ongoing brain activity in the interstimulus intervals (Figure 4A). We found a significantly increased phase locking in the alpha band ($t_{13} = -2.78$, $p < 0.0167$, paired t test, Bonferroni-corrected), but not in the delta/theta band ($t_{13} = -1.70$, $p = 0.11$) or the beta band ($t_{13} = -1.67$, $p = 0.12$). Synchronization to the external driving force should lead to more regular network dynamics during stimulation [2, 13]. We observed that the instantaneous phase angle during the upward zero crossing of the external 10 Hz wave every 3 s (T_0; Figure 1B) across all trials was significantly nonuniformly distributed during stimulation (Rayleigh's test; $p < 0.05$, binomial test), but not during sham (Table S2), indicating that network dynamics followed the external rhythm. We tested whether the increased phase consistency was also preserved throughout the trials by analyzing the averaged inter-trial coherence (ITC; Supplemental Experimental Procedures) before visual stimulus onset (Figure 4C) with paired t tests. We found a significant increase in ITC in the alpha band ($t_{13} = -2.95$, $p < 0.0167$, Bonferroni corrected), but not in the delta/theta band ($t_{13} = 0.8$, $p = 0.44$) or the beta band ($t_{13} = -0.9$, $p = 0.37$). Because the ITC after visual stimulus onset is modulated by prestimulus alpha phase [14, 15], we sorted the data into four phase bins of the ongoing alpha oscillation (Figure 4E). Planned contrasts analysis revealed a relative ITC increase in the alpha band (Figures 4D and 4E) after stimulation when compared to the ITC in the theta ($F_{1,13} = 54.1$, $p < 0.0005$) and

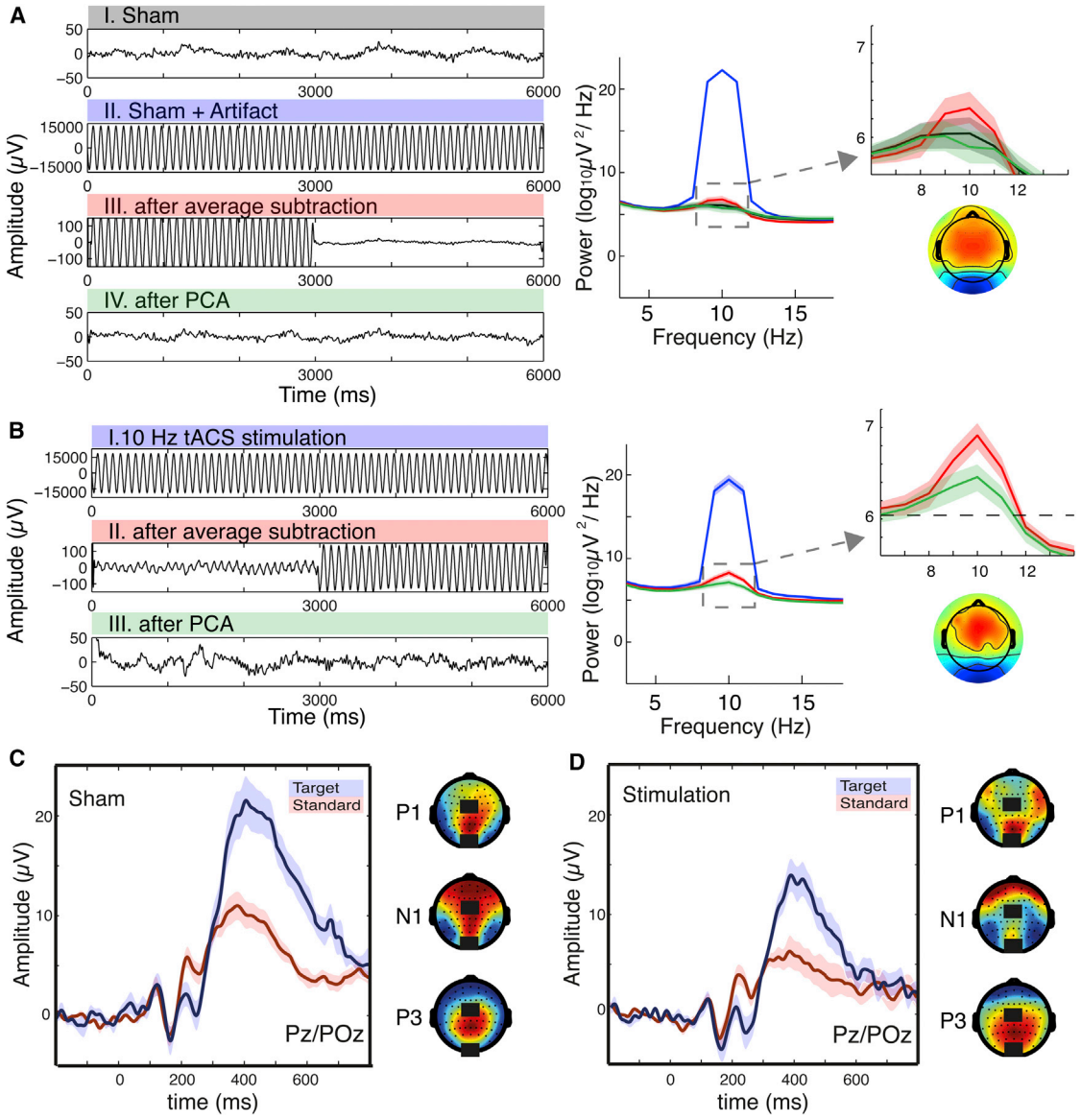

Figure 2. Retrieval of EEG Activity during tACS

(A) Verification of the artifact rejection algorithm. (I) EEG time course for 6000 ms (two trials of one subject) at electrode POz. (II) Same data segment after addition of a constant 10 Hz sine wave. (III) Artifact removal step 1: a moving average template was subtracted from the data revealing that in some trials (e.g., before 3,000 ms), residual artifacts remain. (IV) Step 2: residual artifacts were captured by a PCA and subsequently removed. Plots on the right depict the power spectra for (I)–(IV) across all trials and all subjects (color conventions as in I–IV). The enlarged spectrum on the top right indicates that a residual artifact is still present in the data after the moving average subtraction. After PCA, spectral power is slightly over corrected (green), but the overcorrection did not reach significance. The topography of the typical artifact component is shown below the power spectra.

(B) (I)–(III) depict the same approach for the stimulation data and indicate that the tACS artifact was successfully removed from the recording. Spectral power for (I)–(III); the same color conventions as in (A) apply. The dashed line highlights the spectral peak amplitude of the alpha band in (A).

(C) Grand average ERPs for targets and standards during the sham session along with topographies for the major components: P1, N1, and the P3 at Pz/POz. Values are mean ± SEM.

(D) Grand average ERPs and topographies during stimulation after rejection of the 10 Hz tACS artifact.

See also Figure S1.

the beta band ($F_{1,13} = 212.1$, $p < 0.0005$). Additional results can be found in the Supplemental Information (Table S2).

Behavioral Results

Behavioral data were grouped into four phase bins (specified above, Figure 4E). Target detection accuracy (Figure 4F) was analyzed in a two-way repeated-measures ANOVA with the factors *condition* (sham or stimulation) and *phase* (four bins). We found a significant effect of *condition* ($F_{1,13} = 5.79$, $p < 0.05$) and no effect of the factor *phase* ($F_{2.2,28.1} = 0.2$, $p = 0.8$). However, the interaction of *condition* × *phase* was significant ($F_{2.2,28.5} = 3.37$, $p < 0.05$; Figure 4G), indicating that tACS most likely modulates behavioral performance in a phase-dependent fashion. We found no learning or reaction time effects of the stimulation (all $p > 0.05$; Supplemental Experimental Procedures).

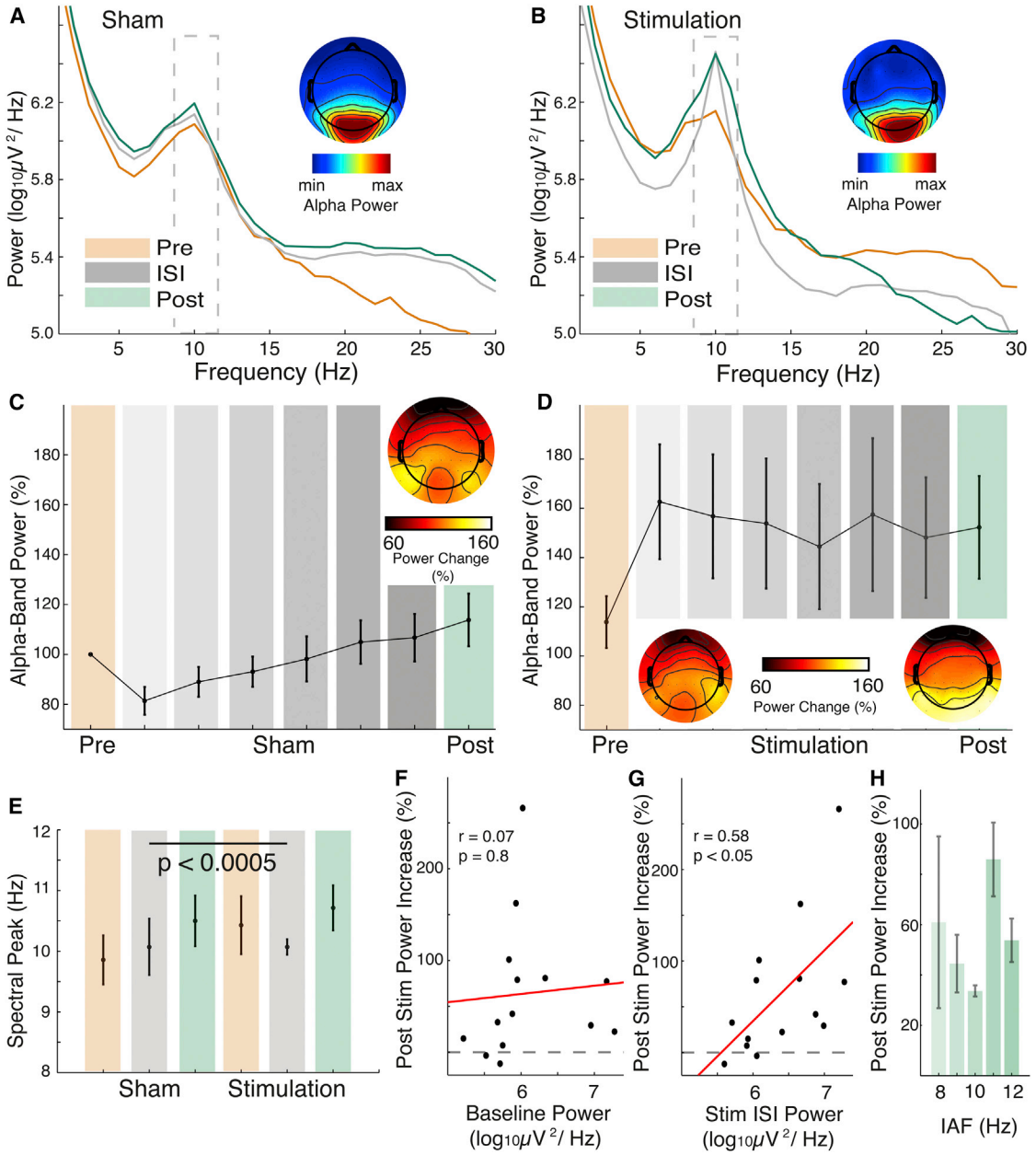

Figure 3. Entrainment of Ongoing Alpha-Band Activity

(A) Grand mean power spectra across all subjects during the sham session (electrode POz). One minute of pre- and postmeasurements were subdivided into 60 segments of 1 s each; the resulting spectra after FFT were averaged. The same procedure was applied to the 400 ISIs (fragmented into 1 s segments). The inset depicts the topography of the alpha-band power (dashed line) during sham.

(B) Grand averages of power spectra during 10 Hz tACS along with pre- and poststimulation measurements (electrode POz).

(C) Average alpha power before, during, and after sham (mean ± SEM) at POz. Values are normalized to the presham baseline power in each subject. The 400 interstimulus interval segments were grouped into six equally distanced grand averages, each containing 60 consecutive spectra sorted with respect to their occurrence during the session. The 40 remaining spectra were discarded. The topography indicates the alpha power change in the postsham measurement relative to the presham baseline.

(D) Average relative alpha power before, during, and after 10 Hz tACS (mean ± SEM). The topographies correspond to the prestimulation and post-stimulation condition and reveal the spatial specific alpha power enhancement after 10 Hz tACS. Note that the power enhancement effect during stimulation outlasts the stimulation period.

(E) Spectral peak analysis of all 14 subjects with a mean IAF of 9.86 Hz ± 0.4 (mean ± SEM). During 10 Hz tACS, the spectral peak is at 10.07 Hz ± 0.1. A Levene's test for equality of variances revealed that the assumption of homoscedasticity was not met during stimulation.

(F) Linear correlation analysis of the absolute alpha power values during presham baseline and the relative poststimulation enhancement in the alpha band revealed no significant interaction. Black dots depict individual subjects.

(G) Linear correlation analysis of the absolute alpha power value observed during stimulation and the relative poststimulation alpha power enhancement revealed a significant interaction.

(H) The IAF was defined as the spectral peak or maximal power value in the presham measurement in the range from 8–12 Hz. The results indicate that the relative alpha power increase after stimulation was not related to the peak frequency before stimulation.

See also Figure S2 and Table S1.

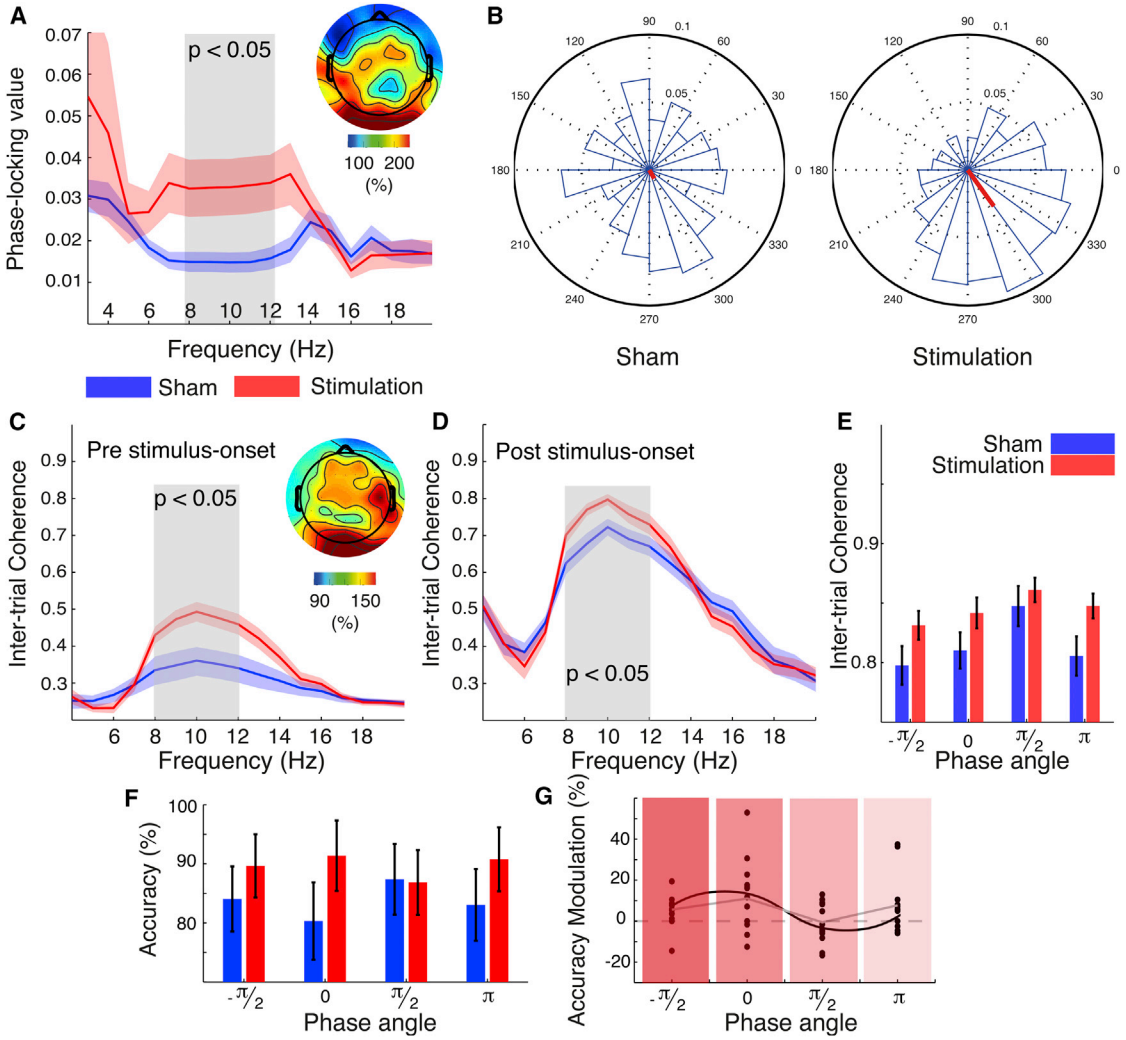

Figure 4. Effects of tACS on Task-Related Responses

(A) Grand mean (±SEM) phase-locking values (PLVs) between the externally applied 10 Hz tACS wave, and the ongoing activity at electrode POz are depicted. For sham, a random 10 Hz sine wave (Figure 2A, II) was used for computation. The gray-shaded area highlights the significant difference (paired t test). The topography on the upper right confirms the spatial specificity of the phase locking increase to parieto-occipital brain areas.

(B) Distribution of instantaneous phase angles at POz in one representative subject across all trials after Hilbert transformation at T_0 (Figure 1B) during the sham (left) and stimulation (right). Single trial data are depicted in blue, the resulting sum vector in red.

(C) Grand mean (±SEM) intertrial coherence was calculated for −500 ms to −200 ms before visual stimulus onset during sham (blue) and during stimulation (red) for four phase angles (see below) separately and then averaged across time points and phase angles. The gray-shaded area delineates the significant difference in the alpha band (paired t test). The topography on the upper right indicates that the ITC increase is confined to parieto-occipital areas.

(D) Poststimulus intertrial coherence (100–200 ms). Grand mean averages (±SEM) for sham and stimulation are depicted. The same conventions as in (C) apply.

(E) Mean (±SEM) poststimulus alpha-band intertrial coherence is depicted for the four phase angles of the underlying alpha oscillation (first bin: −0.75 π to −0.25 π; second bin: −0.25 π to 0.25 π; third bin: 0.25 π to 0.75 π; fourth bin: 0.75 π to −0.75 π; Tick labels depict the center of the respective phase bins) highlighting that alpha ITC is modulated by instantaneous alpha phase. Note that this phase dependency was also present during sham, although ITC was increased during 10 Hz tACS.

(F) Target detection accuracy (mean ± SEM, phase sorting as in E) results relative to the different phase angles for sham (blue) and stimulation (red) revealing higher values during stimulation in three phase bins.

(G) The accuracy modulation (stimulation – sham) was calculated for every subject and every phase bin. Black dots represent individual subjects; the gray line highlights the mean accuracy modulation and is superimposed by a sine wave (black line) indicating the phasic modulation of target detection performance.

See also Table S2.

Discussion

Here, we demonstrate that human oscillatory brain activity as recorded with EEG can be entrained by simultaneous application of tACS. In particular, we show that stimulation at 10 Hz enhances alpha power in the parieto-occipital cortex synchronizes oscillations and modifies behavioral outcome.

Artifact Rejection

The crucial factor in tACS-EEG experiments is the distinction between physiological brain activity and stimulation-induced artifacts, because the frequency of interest is usually equal to the stimulation frequency. We verified our artifact removal approach with a simulation, which strongly supports a successful artifact rejection. (1) Spectral power after artifact rejection on the sham data did not differ significantly from the original sham data (Figures 2AI and 2AIV). (2) Alpha topographies were highly similar during sham and stimulation (Figures 3A, 3B, and S2), indicating that cortical sources of alpha activity were modulated during stimulation. (3) Alpha power during stimulation was significantly correlated with poststimulation power increase (Figure 3G). (4) Increments of power (Figure 3D), phase locking (Figure 4A), and intertrial coherence (Figure 4C) were mainly confined to parieto-occipital areas and the alpha band. (5) The physiological phase-dependent response to the visual stimulus was still present (Figures 4D and 4E; also see evoked power analysis in the Supplemental Experimental Procedures). If residual artifacts were the underlying cause for the phase locking and power increase, a physiological modulation would have been highly unlikely. (6) ERP waveforms and topographies were restored successfully. (7) PCA revealed distinct artifact components (Figure S1).

Physiological Efficacy of tACS

Intracranial recordings in animals demonstrated that spiking activity could be synchronized to different driving frequencies [16] and synchronized to the phase of externally applied alternating currents [17]. So far, electrophysiological evidence in humans was limited to EEG recordings after stimulation [18, 19]. Our data now suggest that (1) 10 Hz tACS increased oscillatory power in the alpha band; (2) the alpha power increase was based on synchronization to the external driving force [2]. (3) 10 Hz tACS transiently shifts the individual alpha peak toward 10 Hz (Figure 3E). This finding has been demonstrated in a modeling study for a 3 Hz network in a frequency range from 2–4.5 Hz [13, 20]; (4) effects of stimulation at 10 Hz are confined to the alpha band. These results agree with a modeling study [21] predicting tACS effects on EEG electrodes and brain activity. However, it remains unresolved whether neuronal entrainment [2] and mechanisms of neural plasticity [19] are the only factors contributing to the outlasting power effect [20]. Importantly, our results reveal that neither baseline power nor the IAF (Figures 3F and 3H) were reliable predictors whether entrainment through 10 Hz tACS was successful (Figure 3G). Complementary modeling approaches will be necessary to individually tailor electrode features (e.g., size or location) and stimulation parameters (e.g., frequency, intensity, phase delay, offset, waveforms [11]) to overcome current limitations of tACS such as the low spatial specificity and the unclear cortical current distribution.

Role of Alpha Oscillations for Visual Perception

In general, alpha is assumed to be a rhythm that can actively suppress processing of irrelevant sensory information and therefore direct information flow to task-relevant neuronal structures (gating by inhibition hypothesis, reviewed in [22–24]). Specifically, it has been demonstrated that high prestimulus alpha power is predictive of decreased visual detection performance in a phase-dependent fashion [15, 25, 26]. Here, we observed a phase-dependent enhancement of target detection performance in states of exogenously boosted alpha activity. Under the assumption that tACS can only entrain cortical oscillators operating close to the driving frequency [2], our results suggest that we successfully modulated the inhibitory alpha network. Furthermore, states of increased alpha phase alignment are predictive of improved memory performance [14] and might facilitate recall performance in an oddball task. In line with the above, previous rTMS experiments on exogenous alpha enhancement described either facilitation [27] or impairment [28] of task performance in different cognitive paradigms. Taken together, our findings imply that exogenously enhanced alpha power reflects increased inhibition of task-irrelevant sites through augmented cortical alpha synchronization.

An unequivocal confirmation on entrainment would be the demonstration that behavioral performance cycles at different frequencies before and after stimulation. However, in contrast to previous reports [29, 30] we did not find a phasic modulation in behavior. A potential confound is the preceding sham session and the slow alpha power increase throughout the task. However, a significant interaction between condition and time demonstrated that the increase was stronger during stimulation (Figure 3D). Outlasting changes after tACS (>30 min [10]) impede an inverse experimental procedure.

Relation to Previous Studies and Implications for Future Studies

Our results extend previous findings and suggest neuronal entrainment as the putative mechanism, which may underlie the previously observed stimulation effects on visual [19, 31–34], somatosensory [35], auditory [18], motor [9, 36–38], and memory systems [7, 39]. This is the first study that combines simulated current flow predictions with electrophysiological and behavioral evidence to demonstrate the efficacy of the stimulation. Our results show that the externally applied electric field does directly influence cortical oscillators in a frequency-specific manner and indicate that tACS can be a powerful tool to investigate neuronal oscillations involved in perceptual and cognitive processing. In the future, tACS might prove to be useful for the clinical application in disorders associated with disturbances of oscillatory signals such as Parkinson's disease [37] or neuropsychiatric disorders [40, 41].

Supplemental Information

Supplemental Information includes Supplemental Experimental Procedures, two figures, and two tables and can be found with this article online at http://dx.doi.org/10.1016/j.cub.2013.12.041.

Acknowledgments

The authors would like to thank Johannes Vosskuhl for help with participant recruitment and data acquisition. This work was supported by grants from the European Union (ERC-2010-AdG-269716, A.K.E.), the German Research Foundation (SFB936/A2/A3/Z1, A.K.E.; RA2357/1-1, S.R.; SFB/TRR 31, C.S.H.), and the German National Academic Foundation (R.F.H.).

Received: June 7, 2013
Revised: November 15, 2013
Accepted: December 17, 2013
Published: January 23, 2014

References

1. Thut, G., Miniussi, C., and Gross, J. (2012). The functional importance of rhythmic activity in the brain. Curr. Biol. *22*, R658–R663.

2. Thut, G., Schyns, P.G., and Gross, J. (2011). Entrainment of perceptually relevant brain oscillations by non-invasive rhythmic stimulation of the human brain. Front. Psychol. *2*, 170.
3. Romei, V., Driver, J., Schyns, P.G., and Thut, G. (2011). Rhythmic TMS over parietal cortex links distinct brain frequencies to global versus local visual processing. Curr. Biol. *21*, 334–337.
4. Thut, G., Veniero, D., Romei, V., Miniussi, C., Schyns, P., and Gross, J. (2011). Rhythmic TMS causes local entrainment of natural oscillatory signatures. Curr. Biol. *21*, 1176–1185.
5. Buzsáki, G., and Draguhn, A. (2004). Neuronal oscillations in cortical networks. Science *304*, 1926–1929.
6. Engel, A.K., Fries, P., and Singer, W. (2001). Dynamic predictions: oscillations and synchrony in top-down processing. Nat. Rev. Neurosci. *2*, 704–716.
7. Polanía, R., Nitsche, M.A., Korman, C., Batsikadze, G., and Paulus, W. (2012). The importance of timing in segregated theta phase-coupling for cognitive performance. Curr. Biol. *22*, 1314–1318.
8. Herrmann, C., Rach, S., Neuling, T., and Strüber, D. (2013). Transcranial alternating current stimulation: a review of the underlying mechanisms and modulation of cognitive processes. Front. Hum. Neurosci *7*, 279.
9. Pogosyan, A., Gaynor, L.D., Eusebio, A., and Brown, P. (2009). Boosting cortical activity at Beta-band frequencies slows movement in humans. Curr. Biol. *19*, 1637–1641.
10. Neuling, T., Rach, S., and Herrmann, C.S. (2013). Orchestrating neuronal networks: sustained after-effects of transcranial alternating current stimulation depend upon brain states. Front. Hum. Neurosci. *7*, 161.
11. Neuling, T., Wagner, S., Wolters, C.H., Zaehle, T., and Herrmann, C.S. (2012). Finite-element model predicts current density distribution for clinical applications of tDCS and tACS. Front. Psychiatry *3*, 83.
12. Polich, J. (2007). Updating P300: an integrative theory of P3a and P3b. Clin. Neurophysiol. *118*, 2128–2148.
13. Ali, M.M., Sellers, K.K., and Fröhlich, F. (2013). Transcranial alternating current stimulation modulates large-scale cortical network activity by network resonance. J. Neurosci. *33*, 11262–11275.
14. Hanslmayr, S., Klimesch, W., Sauseng, P., Gruber, W., Doppelmayr, M., Freunberger, R., and Pecherstorfer, T. (2005). Visual discrimination performance is related to decreased alpha amplitude but increased phase locking. Neurosci. Lett. *375*, 64–68.
15. Hanslmayr, S., Aslan, A., Staudigl, T., Klimesch, W., Herrmann, C.S., and Bäuml, K.-H. (2007). Prestimulus oscillations predict visual perception performance between and within subjects. Neuroimage *37*, 1465–1473.
16. Fröhlich, F., and McCormick, D.A. (2010). Endogenous electric fields may guide neocortical network activity. Neuron *67*, 129–143.
17. Ozen, S., Sirota, A., Belluscio, M.A., Anastassiou, C.A., Stark, E., Koch, C., and Buzsáki, G. (2010). Transcranial electric stimulation entrains cortical neuronal populations in rats. J. Neurosci. *30*, 11476–11485.
18. Neuling, T., Rach, S., Wagner, S., Wolters, C.H., and Herrmann, C.S. (2012). Good vibrations: oscillatory phase shapes perception. Neuroimage *63*, 771–778.
19. Zaehle, T., Rach, S., and Herrmann, C.S. (2010). Transcranial alternating current stimulation enhances individual alpha activity in human EEG. PLoS ONE *5*, e13766.
20. Helfrich, R.F., and Schneider, T.R. (2013). Modulation of cortical network activity by transcranial alternating current stimulation. J. Neurosci. *33*, 17551–17552.
21. Merlet, I., Birot, G., Salvador, R., Molaee-Ardekani, B., Mekonnen, A., Soria-Frish, A., Ruffini, G., Miranda, P.C., and Wendling, F. (2013). From oscillatory transcranial current stimulation to scalp EEG changes: a biophysical and physiological modeling study. PLoS ONE *8*, e57330.
22. Jensen, O., and Mazaheri, A. (2010). Shaping functional architecture by oscillatory alpha activity: gating by inhibition. Front. Hum. Neurosci. *4*, 186.
23. Klimesch, W., Sauseng, P., and Hanslmayr, S. (2007). EEG alpha oscillations: the inhibition-timing hypothesis. Brain Res. Brain Res. Rev. *53*, 63–88.
24. Klimesch, W., Fellinger, R., and Freunberger, R. (2011). Alpha oscillations and early stages of visual encoding. Front. Psychol. *2*, 118.
25. van Dijk, H., Schoffelen, J.-M., Oostenveld, R., and Jensen, O. (2008). Prestimulus oscillatory activity in the alpha band predicts visual discrimination ability. J. Neurosci. *28*, 1816–1823.
26. Mathewson, K.E., Gratton, G., Fabiani, M., Beck, D.M., and Ro, T. (2009). To see or not to see: prestimulus alpha phase predicts visual awareness. J. Neurosci. *29*, 2725–2732.
27. Klimesch, W., Sauseng, P., and Gerloff, C. (2003). Enhancing cognitive performance with repetitive transcranial magnetic stimulation at human individual alpha frequency. Eur. J. Neurosci. *17*, 1129–1133.
28. Romei, V., Gross, J., and Thut, G. (2010). On the role of prestimulus alpha rhythms over occipito-parietal areas in visual input regulation: correlation or causation? J. Neurosci. *30*, 8692–8697.
29. Callaway, E., 3rd, and Yeager, C.L. (1960). Relationship between reaction time and electroencephalographic alpha phase. Science *132*, 1765–1766.
30. de Graaf, T.A., Gross, J., Paterson, G., Rusch, T., Sack, A.T., and Thut, G. (2013). Alpha-band rhythms in visual task performance: phase-locking by rhythmic sensory stimulation. PLoS ONE *8*, e60035.
31. Kanai, R., Chaieb, L., Antal, A., Walsh, V., and Paulus, W. (2008). Frequency-dependent electrical stimulation of the visual cortex. Curr. Biol. *18*, 1839–1843.
32. Kanai, R., Paulus, W., and Walsh, V. (2010). Transcranial alternating current stimulation (tACS) modulates cortical excitability as assessed by TMS-induced phosphene thresholds. Clin. Neurophysiol. *121*, 1551–1554.
33. Brignani, D., Ruzzoli, M., Mauri, P., and Miniussi, C. (2013). Is transcranial alternating current stimulation effective in modulating brain oscillations? PLoS ONE *8*, e56589.
34. Strüber, D., Rach, S., Trautmann-Lengsfeld, S.A., Engel, A.K., and Herrmann, C.S. (2014). Antiphasic 40 Hz oscillatory current stimulation affects bistable motion perception. Brain Topogr. *27*, 158–171.
35. Feurra, M., Paulus, W., Walsh, V., and Kanai, R. (2011). Frequency specific modulation of human somatosensory cortex. Front. Psychol. *2*, 13.
36. Antal, A., Boros, K., Poreisz, C., Chaieb, L., Terney, D., and Paulus, W. (2008). Comparatively weak after-effects of transcranial alternating current stimulation (tACS) on cortical excitability in humans. Brain Stimulat. *1*, 97–105.
37. Brittain, J.-S., Probert-Smith, P., Aziz, T.Z., and Brown, P. (2013). Tremor suppression by rhythmic transcranial current stimulation. Curr. Biol. *23*, 436–440.
38. Feurra, M., Bianco, G., Santarnecchi, E., Del Testa, M., Rossi, A., and Rossi, S. (2011). Frequency-dependent tuning of the human motor system induced by transcranial oscillatory potentials. J. Neurosci. *31*, 12165–12170.
39. Marshall, L., Helgadóttir, H., Mölle, M., and Born, J. (2006). Boosting slow oscillations during sleep potentiates memory. Nature *444*, 610–613.
40. Herrmann, C.S., and Demiralp, T. (2005). Human EEG gamma oscillations in neuropsychiatric disorders. Clin. Neurophysiol. *116*, 2719–2733.
41. Uhlhaas, P.J., and Singer, W. (2010). Abnormal neural oscillations and synchrony in schizophrenia. Nat. Rev. Neurosci. *11*, 100–113.